

RESEARCH ARTICLE | OCTOBER 05 2023

Synthesis and characterization of XeAr_2 under high pressure

FREE

Mengnan Wang ; Mikhail A. Kuzovnikov ; Jack Binns ; Xiaofeng Li; Miriam Peña-Alvarez ; Andreas Hermann ; Eugene Gregoryanz ; Ross T. Howie  

 Check for updates

J. Chem. Phys. 159, 134508 (2023)

<https://doi.org/10.1063/5.0158742>



View
Online



Export
Citation

CrossMark

Articles You May Be Interested In

Argon-neon binary diagram and ArNe_2 Laves phase

J. Chem. Phys. (September 2019)

Single Crystalline Elastic Constants of Cubic MgCu_2 - MgZn_2 Alloys

Journal of Applied Physics (December 2003)

First-principles based computational framework for the thermal conductivity of complex intermetallics: The case study of MgZn_2 and Mg_4Zn_7

J. Appl. Phys. (January 2023)

500 kHz or 8.5 GHz?
And all the ranges in between.

Lock-in Amplifiers for your periodic signal measurements



Find out more

 Zurich
Instruments

Synthesis and characterization of XeAr₂ under high pressure

Cite as: J. Chem. Phys. 159, 134508 (2023); doi: 10.1063/5.0158742

Submitted: 17 May 2023 • Accepted: 13 September 2023 •

Published Online: 5 October 2023



Mengnan Wang,¹ Mikhail A. Kuzovnikov,¹ Jack Binns,² Xiaofeng Li,³ Miriam Peña-Alvarez,¹ Andreas Hermann,¹ Eugene Gregoryanz,^{1,2,4} and Ross T. Howie^{1,2,a)}

AFFILIATIONS

¹Centre for Science at Extreme Conditions and School of Physics and Astronomy, University of Edinburgh, Edinburgh, United Kingdom

²Center for High Pressure Science and Technology Advanced Research, Shanghai, China

³College of Physics and Electronic Information, Luoyang Normal University, Luoyang, China

⁴Key Laboratory of Materials Physics, Institute of Solid State Physics, CAS, Hefei, China

^{a)}Author to whom correspondence should be addressed: ross.howie@ed.ac.uk

ABSTRACT

The binary Xe–Ar system has been studied in a series of high pressure diamond anvil cell experiments up to 60 GPa at 300 K. *In-situ* x-ray powder diffraction and Raman spectroscopy indicate the formation of a van der Waals compound, XeAr₂, at above 3.5 GPa. Powder x-ray diffraction analysis demonstrates that XeAr₂ adopts a Laves MgZn₂-type structure with space group *P6₃/mmc* and cell parameters $a = 6.595 \text{ \AA}$ and $c = 10.716 \text{ \AA}$ at 4 GPa. Density functional theory calculations support the structure determination, with agreement between experimental and calculated Raman spectra. Our DFT calculations suggest that XeAr₂ would remain stable without a structural transformation or decomposition into elemental Xe and Ar up to at least 80 GPa.

Published under an exclusive license by AIP Publishing. <https://doi.org/10.1063/5.0158742>

I. INTRODUCTION

The simple closed-shell electronic configurations make the rare gases and their mixtures ideal cases to compare experiment and theory.¹ It was long believed that the rare gases were chemically inert. However, since the 1960s, stable halide and oxide xenon compounds XeF₄,² XeF₆,³ and XeO₄⁴ have been synthesized through powerful oxidizing agents, O₂ and F₂. With the application of pressure, a variety of rare-gas van der Waals compounds have been produced, such as Ar(H₂)₂,⁵ Kr(H₂)₄,⁶ Xe(H₂)₇,⁷ and Xe(N₂)₂.⁸ As such, dense rare gases (RGs) can be considered archetypical cases to understand van der Waals interactions.⁹

Aside from helium, all heavier rare gases crystallize in a face-centered cubic (*fcc*) crystal structure at ambient pressure and low temperature. At room temperature, upon compression, they undergo a sluggish *fcc* to hexagonal close-packed (*hcp*) martensitic transition with a wide pressure regime of coexistence. The onset of the *fcc*-to-*hcp* transition is above 20 GPa in Ar,¹⁰ 3.2 GPa in Kr,¹¹ and 1.5 GPa in Xe.¹² The mechanism for the coexistence of *fcc* and *hcp* phases for heavier rare gases remains unclear. One theory suggests

that the stabilization of the *hcp* structure is caused by the hybridization between the *s*, *p* valence bands and the *d* band.¹³ Among all the rare gases, xenon is the only one that was shown experimentally to become a metal above 135 GPa^{14–16} and is predicted to be superconducting at higher pressure.¹⁷

High pressure can dramatically enhance chemical reactivity, enabling the formation of compounds that do not exist at ambient conditions. Due to their simplicity and inert chemical behavior caused by closed-shell electronic configurations, rare gases are not known to react with one another but can form van der Waals compounds under compression. The majority of van der Waals compounds crystallize in one of the following Laves-type phases with AB₂ composition: MgCu₂ (cubic with 24 atoms in the unit cell), MgZn₂ (hexagonal with 12 atoms in the unit cell), or MgNi₂ (hexagonal with 24 atoms in the unit cell).^{18–20} Laves phases consist of large A and small B atoms arranged in a way to maximize packing density. Typically, the ratios of atomic radii r_A/r_B in Laves phases are close to 1.2:1 (this value varies from 1.05 to 1.7 under extreme conditions).²¹ AB₂ compounds with r_A/r_B radii ratio slightly smaller than 1.2 usually crystallize in a hexagonal MgZn₂-type structure. The

cubic MgCu_2 -type Laves phase is favored when the atomic diameters r_A/r_B have a ratio slightly larger than 1.2.²¹

Among binary mixtures of rare gases, only the light mixtures, Ne–He and Ar–Ne have been experimentally explored, forming NeHe_2 ²² and ArNe_2 ,²³ respectively. NeHe_2 was the first compound reported in the RG–RG binary system. With a radii ratio of 1.19 of its constituent atoms at 15 GPa, this compound has a MgZn_2 -type Laves phase structure (space group $P6_3/mmc$), with helium and neon occupying the $2a+6h$ and $4f$ sites, respectively. NeHe_2 remains stable up to 90 GPa, and its bulk modulus is bigger than He while smaller than Ne.²⁴ Another stoichiometric compound ArNe_2 adopts the same structure with $r_{\text{Ar}}/r_{\text{Ne}} = 1.228$ at 6 GPa. The bulk modulus of ArNe_2 also lies in between its constituent elements and remains stable up to 65 GPa.²³ However, a recent first-principles study predicted that the comparatively heavier Xe–Ar binary noble gas system would behave differently, instead forming a MgCu_2 -type Laves phase structure at pressures above 1.1 GPa.²⁵

In this paper, we report the formation of the van der Waals compound, XeAr_2 , at 300 K and 3.5 GPa. Synchrotron x-ray diffraction demonstrates that XeAr_2 adopts a MgZn_2 -type crystal structure with cell parameters $a = 6.595 \text{ \AA}$ and $c = 10.715 \text{ \AA}$ at 4 GPa. Our DFT calculations indicate that XeAr_2 would be stable without any phase transition or decomposition for at least up to 80 GPa.

II. EXPERIMENTAL DETAILS

High purity Xe (BOC, 99.99%) was initially cryogenically loaded as a solid into diamond anvil cells (DACs) under a nitrogen atmosphere below 161 K. After the temperature was quenched, loading was confirmed by the change in refractive index between the empty and loaded DAC. High purity argon (BOC, 99.998%) was subsequently gas loaded into the sample chamber at 0.2 GPa, partially substituting Xe.^{26,27} Due to the inherent complexity of the gas loading procedure, the exact Xe/Ar sample ratio could not be controlled. However, both our Raman and XRD data suggest an excess of Xe in the Xe–Ar system. Diamonds with a culet diameter of 200 μm were used to generate pressure in all experiments, and rhenium foil was used as the gasket material. Raman spectroscopy was initially used to rule out possible contamination after sample loading and to identify compound formation. Raman measurements were performed using a custom-built confocal Raman system with a 514 nm excitation wavelength of an Ar^+ ion laser with a laser power of 32 mW. Powder x-ray diffraction data were collected at P02.2 at PETRA-III (Germany), and incident beam energies in a range of 25–30 keV were used. Pressure was determined from the equation of state of Au²⁸ for synchrotron x-ray diffraction measurements and ruby fluorescence for Raman spectroscopy measurements (Fig. 1, inset).²⁹ Calibration of the sample-detector distance, primary processing, azimuthal integration, and background subtraction were performed using the DIOPTAS 0.5.5 software.³⁰ Indexing was carried out using GSAS-II,³¹ while the Rietveld refinements were done in POWDERCELL 2.4,³² and the equations of state data were determined using EoSFIT7.³³

Total energy calculations were carried out within the framework of density functional theory (DFT) in conjunction with the projector-augmented wave (PAW) method and a plane wave basis, as implemented in the VASP code.³⁴ We used the RPBE exchange-correlation functional³⁵ and standard PAW data sets (cutoff radii:

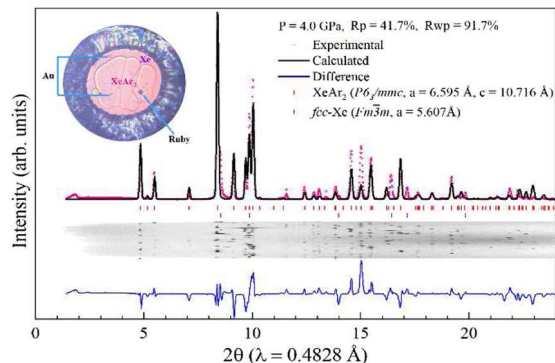


FIG. 1. Powder x-ray diffraction pattern ($\lambda = 0.4828 \text{ \AA}$) of XeAr_2 obtained from the Xe–Ar mixture at 4 GPa with its Rietveld refinement. Two solid phases (XeAr_2 and fcc-Xe) are observed in the system. XeAr_2 adopts a hexagonal ($P6_3/mmc$) unit cell with $a = 6.595 \text{ \AA}$, $c = 10.716 \text{ \AA}$, and fcc-Xe ($Fm-3m$) with $a = 5.607 \text{ \AA}$. Top left inset: photomicrograph of the XeAr_2 crystals embedded in Xe at 4 GPa; arrows indicate the pressure marker Au (for x-ray diffraction measurements) and ruby sphere (for Raman measurements). Bottom inset: a cake representation of the diffraction pattern.

$r_{\text{Xe}} = 2.5 a_B$, $r_{\text{Ar}} = 1.9 a_B$) that include eight electrons in the valence space for each element. The MgCu_2 , MgZn_2 , and MgNi_2 structure types were fully optimized at a series of pressures up to 80 GPa, until the remaining force components were below 2 meV/ \AA (0.5 meV/ \AA for the MgZn_2 structure). The plane wave cutoff energy was 400 eV and Brillouin zone sampling was done on regular k -point grids with a separation of 0.05 \AA^{-1} . Phonon dispersions, densities of states (DOS's), and Raman intensities were obtained using the finite displacement method in suitable supercells, combining VASP with the phonopy and phonopy-spectroscopy packages.^{36,37}

III. RESULTS AND DISCUSSION

At room temperature, argon solidifies at 1.3 GPa,^{38,39} adopting the fcc configuration, while Xe crystallizes at 0.42 GPa with the same structure.⁴⁰ Xenon and argon are miscible in the mixed fluid phase after loading at 0.8 GPa, and no Raman activity could be observed up to 3.0 GPa [Fig. 3(c)]. At a pressure of 3.5 GPa, the mixture visibly phase separated into two solids (Fig. 1 inset), one of which exhibited Raman activity [Fig. 3(c)]. The solidification pressure is higher than the solidification pressure of both constituent elements and is most likely dependent on the initial Xe:Ar mixture concentration. X-ray diffraction analysis reveals the formation of a new Xe–Ar van der Waals compound, XeAr_2 . In all samples, XeAr_2 was phase separated from Xe (top inset to Fig. 1). The XRD pattern of this compound indicates that it possesses the MgZn_2 -type crystal structure with $a = 6.595 \text{ \AA}$ and $c = 10.716 \text{ \AA}$ at 4 GPa, which is shown in the inset in Fig. 2(b). The results of the Rietveld refinement of this crystal structure are displayed in Fig. 1. The effects of the coarse grain powder samples prevented us from refining the atomic coordinates, which were inferred from the parent MgZn_2 structural type and fixed during the refinements.²¹ Our DFT calculations support this structure attribution (see below). The atomic coordinates of Xe and Ar atoms, optimized by DFT at 10 GPa, are indicated in Table S1.

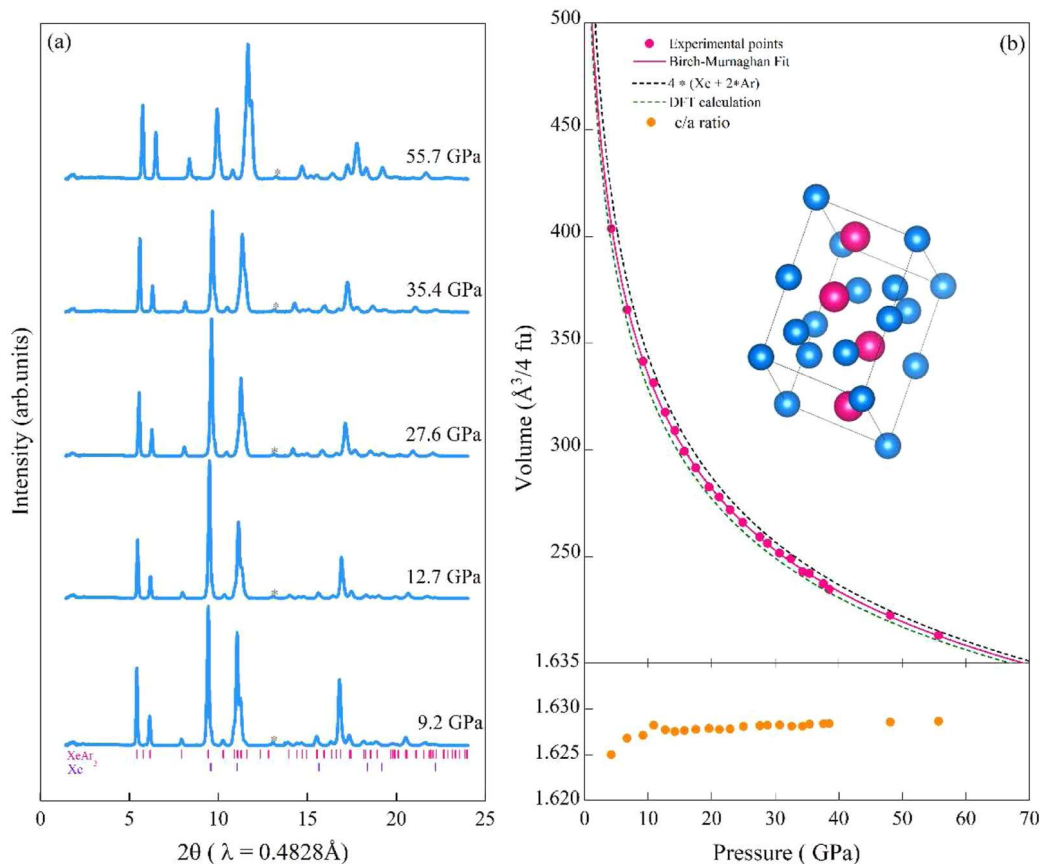


FIG. 2. (a): High-pressure x-ray diffraction patterns ($\lambda = 0.4828 \text{ \AA}$) of XeAr_2 to 55.7 GPa on compression at room temperature. Asterisks correspond to Re gaskets. The pressures were determined from the equation of state of Au. The pink and purple ticks indicate the calculated peak positions for hexagonal XeAr_2 and fcc-Xe, respectively. (b): volume per four formula units as a function of pressure. Pink circles are the experimental data for XeAr_2 (the error bars are smaller than the symbol size). The pink curve represents the fit of the $V(P)$ data for XeAr_2 by the third-order Birch–Murnaghan equation of state with the parameters listed in the supplementary material Table I. The green dashed line represents the volume as a function of pressure derived from our DFT calculations, and the black dashed lines are the volumes of ideal mixtures of $4 \times V_{\text{Xe}} + 8 \times V_{\text{Ar}}$ using the previously determined equations of state of pure Xe and Ar.^{12,38} Top inset: crystal-structure of the Laves phase XeAr_2 , where the Xe atoms (pink spheres) and the Ar (blue spheres) occupy the Mg (4f) and Zn (2a+6h) sites, respectively. Bottom inset: the experimental c/a ratio of XeAr_2 as a function of pressure.

We find XeAr_2 remains stable with no phase transition in the studied pressure range [see Fig. 2(a)]. The unit cell volume and cell parameters of XeAr_2 shift smoothly with increasing pressure, as shown in Fig. 2(b), suggesting no change in stoichiometry or decomposition to elemental Xe and Ar up to 60 GPa. The experimental volumes of XeAr_2 are slightly bigger than those of the DFT calculations at the same pressure. The volume of the cell, 331.441 \AA^3 is 2.6% lower than a volume of $8 \times \text{Ar} + 4 \times \text{Xe}$ at the same pressure, 10.9 GPa, indicating no chemical interaction between xenon and argon.^{12,39} There is good agreement between the experimental and theoretically derived volumes [green dashed line in Fig. 2(b)]. The volume per 4 formula as a function of pressure of XeAr_2 from experiment, XeAr_2 from DFT calculation, and a literature value of $4 \times (\text{Xe} + 2 \text{ Ar})$ are fitted with the third-order Birch–Murnaghan P–V equation of states [see Fig. 2(b)] with the fit parameters shown in Table S2. Estimated from the equation of state of

xenon and argon, the radius ratio varies from 1.15 to 1.2 between 6 and 100 GPa.^{12,39}

The bulk moduli of XeAr_2 are slightly smaller than pure Xe but bigger than pure Ar. In addition, the c/a ratio is close to the ideal value of $\sqrt{8/3}$ for hexagonal structure (Fig. 2 inset).

Our DFT calculations support the structural assignment, as the MgZn_2 structure type is the energetically most favored Laves type structure for XeAr_2 at all pressures (supplementary material Figs. S1 and S2). Its calculated pressure–volume relation is close to, but systematically below, the experimental data, see Fig. 2. While there is a thermal expansion discrepancy between the DFT data (calculated in the ground state) and the XRD (measured at room temperature), this can not account alone for this difference, as the role of thermal effects should decrease with increasing pressure. Since there is no chemical bonding in this compound, its compressibility is determined solely by Pauli repulsion and, therefore, depends

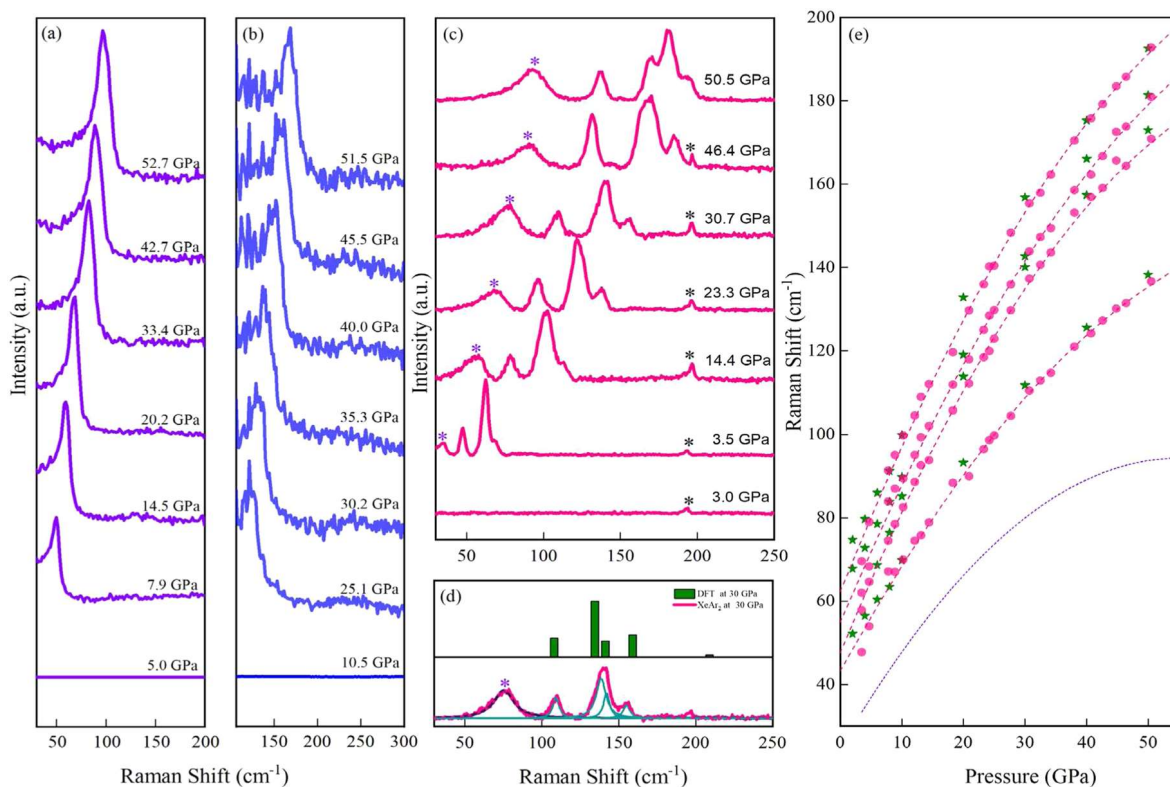


FIG. 3. Representative Raman spectra of pure Xe, Ar, and their mixtures. (a) Raman spectra of pure xenon as a function of pressure. (b) Raman spectra of pure argon as a function of pressure. (c) Raman spectra of XeAr₂ on decompression: purple asterisks indicate the mode corresponding to excess Xe in the sample chamber, while the gray asterisks indicate a peak that does not emanate from the sample. (d) Comparison between the experimental Raman spectra (lower) and the Raman spectra obtained from DFT calculations (top) at 30 GPa. (e) Vibrational frequencies of XeAr₂ as a function of pressure. Pink solid circles correspond to the 4 experimentally measured Raman modes of XeAr₂, and green stars are the Raman frequencies derived from DFT calculations. The purple dash dotted curve is the Raman frequency of excess Xe. Pink dashed thin lines are the fittings to the experimental data.

on how accurately the DFT functional describes the closed shell electron distribution of both Xe and Ar. We conjecture that the RPBE functional produces atoms that are slightly “smaller” and “softer” than they should be, therefore artificially increasing the density and compressibility of XeAr₂.

We have performed Raman spectroscopy experiments on both pure xenon and pure argon up to 50 GPa at room temperature to provide a comparison with their mixtures. There are no Raman-active modes for *fcc* xenon and argon; however, upon the transformation to the *hcp* phase, the transverse optic E_{2g} phonon mode could be observed [see Figs. 3(a) and 3(b)]. The onset of the E_{2g} phonon mode of *hcp*-Xe appears at 7.9 GPa with a frequency of 50 cm⁻¹, reaching 97 cm⁻¹ at 52.7 GPa. Whilst, the argon E_{2g} phonon mode appears at 20.1 GPa with a frequency of 111 cm⁻¹, and its Raman frequency increases with pressure to 169 cm⁻¹ at 51.5 GPa. The Raman intensity of the E_{2g} mode increases with pressure for both xenon and argon, which results from a gradual increase in the relative fraction of the *hcp* phase in a two-phase *fcc* + *hcp* mixture. This is in very good agreement with previous experimental and theoretical work.^{41,42}

The Raman modes of XeAr₂ appear upon solidification of the mixture. The Raman spectrum consists of four resolvable modes as shown in Fig. 3(c). At 3.5 GPa, the lowest-frequency mode (predicted to be at a frequency of 40 cm⁻¹) overlaps with that of pure Xe at the same conditions; however, this becomes resolvable at higher pressure.

Our DFT calculations yield a total of 7 Raman active modes of XeAr₂, with 4 of these observed in experiments. The remaining calculated modes have intensities an order of magnitude lower than the others; hence, they were not observed in the experiments (Fig. S3). Figure 3(d) shows the experimental Raman spectra (lower) and the fitted peak intensities compared with theoretical DFT intensities (top) at 30 GPa. The pressure dependencies of the frequencies obtained in the experiments and the theoretical DFT calculation are in very good agreement with each other. There is no imaginary frequency for all cases, which demonstrates dynamic stability for all pressures we studied (Fig. S3). The frequencies of all the Raman modes harden with pressure; however, interestingly, the lowest E_{2g} is predicted to monotonically decrease with a pressure of above 50 GPa.

Previous first-principle calculation studies on the Ar–He and Xe–Ar systems predict both to form Laves phases adopting the MgCu_2 -type structure.^{25,43} However, experimental studies contradict this, with the two previous reported RG–RG Laves phase compounds, ArHe_2 and NeHe_2 , and that reported here, XeAr_2 , all adopting the MgZn_2 -type structure.^{22,23} Interestingly, binary mixtures of hard spheres are predicted to initially form Laves phases and subsequently decompose into pure end-members at high pressure.⁴⁴ In contrast, our DFT calculations show good agreement with experimental results, suggesting that the stability of XeAr_2 increases with pressure, and we rule out decomposition into elemental Xe and Ar up to 80 GPa.

IV. CONCLUSIONS

In summary, we have explored the Xe–Ar system up to a pressure of 60 GPa with combined Raman spectroscopy, x-ray diffraction, and first-principle DFT calculations. A novel van der Waals compound XeAr_2 has been observed at 3.5 GPa. We find that pressure stabilizes the formation of a stoichiometric, solid van der Waals compound of composition XeAr_2 . Synchrotron x-ray diffraction shows that this compound adopts a MgZn_2 -type crystal structure, which is a Laves phase. Our DFT calculation on formation enthalpy indicates XeAr_2 would be stable without any phase transition or decomposition up to at least 80 GPa.

SUPPLEMENTARY MATERIAL

The supplementary material includes the third-order Birch–Murnaghan EoS fitting parameters, atomic coordinates optimized by DFT at 10 GPa, relative harmonic vibrational free energies as a function of temperature, volumes for XeAr_2 at a certain pressure obtained from over 15 different exchange–correlation functionals, formation enthalpies, simulated Raman spectra of XeAr_2 , and DFT–PBE phonon dispersions.

ACKNOWLEDGMENTS

M.P.-A. acknowledges the support of the UKRI Future Leaders Fellowship No. Mrc-Mr/T043733/1. R.T.H. acknowledges that the project has received funding from the European Research Council (ERC) under the European Union’s Horizon 2020 research and innovation program (Grant Agreement No. 948895 “MetElOne”). We acknowledge DESY (Hamburg, Germany), a member of the Helmholtz Association HGF, for the provision of experimental facilities. Parts of this research were carried out at PETRA-III, and we thank H.-P.Liermann and N. Giordano for assistance in using beamline P02.2 (No. I-20191366). Computational resources provided by the UK’s National Supercomputer Service through the UK Car-Parrinello HEC consortium (EP/X035891/1) are gratefully acknowledged.

AUTHOR DECLARATIONS

Conflict of Interest

The authors have no conflicts to disclose.

Author Contributions

Mengnan Wang: Data curation (lead); Formal analysis (lead); Investigation (equal); Writing – original draft (lead). **Mikhail A. Kuzovnikov:** Data curation (equal); Formal analysis (equal); Writing – review & editing (equal). **Jack Binns:** Formal analysis (equal); Writing – review & editing (equal). **Xiaofeng Li:** Formal analysis (equal); Software (equal). **Miriam Peña-Alvarez:** Data curation (equal); Investigation (equal). **Andreas Hermann:** Formal analysis (equal); Software (equal). **Eugene Gregoryanz:** Formal analysis (equal); Resources (equal); Supervision (equal); Writing – review & editing (equal). **Ross T. Howie:** Conceptualization (equal); Supervision (equal); Writing – original draft (equal); Writing – review & editing (equal).

DATA AVAILABILITY

The majority of the data that support the findings are available within the manuscript. The raw experimental data are available from the corresponding author upon reasonable request.

REFERENCES

- 1 M. L. Klein, J. A. Venables, and J. Venables, *Rare gas solids* (Academic Press, 1976), Vol. 1.
- 2 N. Bartlett, Xenon hexafluoroplatinate (v) $\text{Xe}^+ [\text{Pt}(\text{F}_6)]^-$ (1962).
- 3 H. Selig, H. H. Claassen, C. L. Chernick, J. G. Malm, and J. L. Huston, “Xenon tetroxide: Preparation and some properties,” *Science* **143**, 1322–1323 (1964).
- 4 A. Dewaele, N. Worth, C. J. Pickard, R. J. Needs, S. Pascarelli, O. Mathon, M. Mezouar, and T. Irifune, “Synthesis and stability of xenon oxides Xe_2O_5 and Xe_3O_2 under pressure,” *Nat. Chem.* **8**, 784–790 (2016).
- 5 C. Ji, A. F. Goncharov, V. Shukla, N. K. Jena, D. Popov, B. Li, J. Wang, Y. Meng, V. B. Prakapenka, J. S. Smith *et al.*, “Stability of $\text{Ar}(\text{H}_2)_2$ to 358 GPa,” *Proc. Natl. Acad. Sci. U. S. A.* **114**, 3596–3600 (2017).
- 6 A. K. Kleppe, M. Amboage, and A. P. Jephcoat, “New high-pressure van der Waals compound $\text{Kr}(\text{H}_2)_4$ discovered in the krypton–hydrogen binary system,” *Sci. Rep.* **4**, 4989 (2014).
- 7 M. Somayazulu, P. Dera, A. F. Goncharov, S. A. Gramsch, P. Liermann, W. Yang, Z. Liu, H.-k. Mao, and R. J. Hemley, “Pressure-induced bonding and compound formation in xenon–hydrogen solids,” *Nat. Chem.* **2**, 50–53 (2010).
- 8 R. T. Howie, R. Turnbull, J. Binns, M. Frost, P. Dalladay-Simpson, and E. Gregoryanz, “Formation of xenon–nitrogen compounds at high pressure,” *Sci. Rep.* **6**, 34896 (2016).
- 9 C. Gough, *Introduction to Solid State Physics*, 6th ed. (IOP Publishing, 1986).
- 10 H. Shimizu, M. Kawajiri, T. Kume, S. Sasaki, Y. A. Freiman, and S. M. Tretyak, “High-pressure fcc-to-hcp phase transition in solid krypton studied by Raman spectroscopy,” *Phys. Rev. B* **79**, 132101 (2009).
- 11 D. Errandonea, B. Schwager, R. Boehler, and M. Ross, “Phase behavior of krypton and xenon to 50 GPa,” *Phys. Rev. B* **65**, 214110 (2002).
- 12 H. Cynn, C. Yoo, B. Baer, V. Iota-Herbei, A. McMahan, M. Nicol, and S. Carlson, “Martensitic fcc-to-hcp transformation observed in xenon at high pressure,” *Phys. Rev. Lett.* **86**, 4552 (2001).
- 13 A. McMahan, “Structural transitions and metallization in compressed solid argon,” *Phys. Rev. B* **33**, 5344 (1986).
- 14 K. A. Goettel, J. H. Eggert, I. F. Silvera, and W. C. Moss, “Optical evidence for the metallization of xenon at 132(5) GPa,” *Phys. Rev. Lett.* **62**, 665 (1989).
- 15 M. Ross and A. McMahan, “Condensed xenon at high pressure,” *Phys. Rev. B* **21**, 1658 (1980).
- 16 A. Ray, S. Trickey, R. Weidman, and A. B. Kunz, “Lattice constant at the insulator–metal transition of crystalline xenon,” *Phys. Rev. Lett.* **45**, 933 (1980).
- 17 Y. Yao and J. S. Tse, “Electron–phonon coupling in the high-pressure hcp phase of xenon: A first-principles study,” *Phys. Rev. B* **75**, 134104 (2007).

- ¹⁸F. Laves, *Theory of Alloy Phases* (American Society for Metals Symposium, Cleveland, OH, 1956), p. 124.
- ¹⁹R. L. Johnston and R. Hoffmann, "Structure-bonding relationships in the laves phases," *Z. Anorg. Allg. Chem.* **616**, 105–120 (1992).
- ²⁰B. L. Blaney and G. E. Ewing, "Van der Waals molecules," *Annu. Rev. Phys. Chem.* **27**, 553–584 (1976).
- ²¹F. Stein, M. Palm, and G. Sauthoff, "Structure and stability of laves phases. Part I. Critical assessment of factors controlling laves phase stability," *Intermetallics* **12**, 713–720 (2004).
- ²²P. Loubeyre, M. Jean-Louis, R. LeToullec, and L. Charon-Gérard, "High pressure measurements of the He-Ne binary phase diagram at 296 K: Evidence for the stability of a stoichiometric NeHe₂ solid," *Phys. Rev. Lett.* **70**, 178–181 (1993).
- ²³A. Dewaele, A. D. Rosa, and N. Guignot, "Argon-neon binary diagram and ArNe₂ laves phase," *J. Chem. Phys.* **151**, 124708 (2019).
- ²⁴H. Fukui, N. Hirao, Y. Ohishi, and A. Q. Baron, "Compressional behavior of solid NeHe₂ up to 90 GPa," *J. Phys.: Condens. Matter* **22**, 095401 (2010).
- ²⁵X. Z. Yan, Y. M. Chen, and H. Y. Geng, "Prediction of the reactivity of argon with xenon under high pressures," *ACS Omega* **4**, 13640–13644 (2019).
- ²⁶R. T. Howie, P. Dalladay-Simpson, and E. Gregoryanz, "Raman spectroscopy of hot hydrogen above 200 GPa," *Nat. Mater.* **14**, 495–499 (2015).
- ²⁷P. Dalladay-Simpson, R. T. Howie, and E. Gregoryanz, "Evidence for a new phase of dense hydrogen above 325 gigapascals," *Nature* **529**, 63–67 (2016).
- ²⁸D. L. Heinz and R. Jeanloz, "The equation of state of the gold calibration standard," *J. Appl. Phys.* **55**, 885–893 (1984).
- ²⁹H. Mao, J.-A. Xu, and P. Bell, "Calibration of the ruby pressure gauge to 800 kbar under quasi-hydrostatic conditions," *J. Geophys. Res.* **91**, 4673–4676, <https://doi.org/10.1029/jb091ib05p04673> (1986).
- ³⁰C. Prescher and V. B. Prakapenka, "Dioptas: A program for reduction of two-dimensional x-ray diffraction data and data exploration," *High Pressure Res.* **35**, 223–230 (2015).
- ³¹B. H. Toby and R. B. Von Dreele, "GSAS-II: The genesis of a modern open-source all purpose crystallography software package," *J. Appl. Crystallogr.* **46**, 544–549 (2013).
- ³²W. Kraus and G. Nolze, "POWDER CELL—A program for the representation and manipulation of crystal structures and calculation of the resulting X-ray powder patterns," *J. Appl. Crystallogr.* **29**, 301–303 (1996).
- ³³J. Gonzalez-Platas, M. Alvaro, F. Nestola, and R. Angel, "EosFit7-GUI: A new graphical user interface for equation of state calculations, analyses and teaching," *J. Appl. Crystallogr.* **49**, 1377–1382 (2016).
- ³⁴G. Kresse and J. Furthmüller, "Efficient iterative schemes for *ab initio* total-energy calculations using a plane-wave basis set," *Phys. Rev. B* **54**, 11169–11186 (1996).
- ³⁵J. P. Perdew, K. Burke, and M. Ernzerhof, "Generalized gradient approximation made simple," *Phys. Rev. Lett.* **77**, 3865–3868 (1996).
- ³⁶A. Togo and I. Tanaka, "First principles phonon calculations in materials science," *Scr. Mater.* **108**, 1–5 (2015).
- ³⁷J. M. Skelton, L. A. Burton, A. J. Jackson, F. Oba, S. C. Parker, and A. Walsh, "Lattice dynamics of the tin sulphides SnS₂, SnS and Sn₂S₃: Vibrational spectra and thermal transport," *Phys. Chem. Chem. Phys.* **19**, 12452–12465 (2017).
- ³⁸M. Ross, H. Mao, P. Bell, and J. Xu, "The equation of state of dense argon: A comparison of shock and static studies," *J. Chem. Phys.* **85**, 1028–1033 (1986).
- ³⁹D. Errandonea, R. Boehler, S. Japel, M. Mezouar, and L. Benedetti, "Structural transformation of compressed solid Ar: An x-ray diffraction study to 114 GPa," *Phys. Rev. B* **73**, 092106 (2006).
- ⁴⁰W. A. Caldwell, J. H. Nguyen, B. G. Pfommer, F. Mauri, S. G. Louie, and R. Jeanloz, "Structure, bonding, and geochemistry of xenon at high pressures," *Science* **277**, 930–933 (1997).
- ⁴¹Y. A. Freiman, A. F. Goncharov, S. M. Tretyak, A. Grechnev, J. S. Tse, D. Errandonea, H.-K. Mao, and R. J. Hemley, "Raman scattering in hcp rare gas solids under pressure," *Phys. Rev. B* **78**, 014301 (2008).
- ⁴²H. Shimizu, N. Wada, T. Kume, S. Sasaki, Y. Yao, and J. S. Tse, "Pressure-induced structural transformation in solid xenon studied by Raman spectroscopy," *Phys. Rev. B* **77**, 052101 (2008).
- ⁴³C. Cazorla, D. Errandonea, and E. Sola, "High-pressure phases, vibrational properties, and electronic structure of NeHe₂ and ArHe₂: A first-principles study," *Phys. Rev. B* **80**, 064105 (2009).
- ⁴⁴A.-P. Hynninen, L. Filion, and M. Dijkstra, "Stability of LS and LS₂ crystal structures in binary mixtures of hard and charged spheres," *J. Chem. Phys.* **131**, 064902 (2009).